Samuel, N. K. P., Singh, M., Yamaguchi, K., & Regen, S L. (1985) *J. Am. Chem. Soc. 107*, 42–47.
Selinger, Z., & Lapidot, Y. (1966) *J. Lipid Res. 7*, 174.
Sharkey, N. A., & Blumberg, P. M. (1985) *Cancer Res. 45*, 19–24.
Shirley, D. A. (1949) *Org. React. (N.Y.) 8*, 28–58.
Shoji, M., Vogler, W. R., & Kuo, J. F. (1985) *Biochem. Biophys. Res. Commun. 127*, 590–595.
Takai, Y., Kishimoto, A., Iwasa, Y., Kawahara, Y., Mori, T., & Nishizuka, Y. (1979) *J. Biol. Chem. 254*, 3692–3695.
Wise, B. C., Raynor, R. L., & Kuo, J. F. (1982) *J. Biol. Chem. 257*, 8481–8488.

Influence of Head-Group Interactions on the Miscibility of Synthetic, Stereochemically Pure Glycolipids and Phospholipids†

R. D. Koynova,‡ H. L. Kuttenreich,§ B. G. Tenchov,‡ and H.-J. Hinz*,§

Central Laboratory of Biophysics, Bulgarian Academy of Sciences, Sofia 1113, Bulgaria, and Institut für Biophysik und Physikalische Biochemie, Universität Regensburg, D-8400 Regensburg, West Germany

Received June 26, 1987; Revised Manuscript Received December 4, 1987

ABSTRACT: Phase diagrams of binary mixtures of the glycoglycerolipids 1,2-di-*O*-tetradecyl-3-*O*-β-D-galactosyl-*sn*-glycerol (14-Gal) and 1,2-di-*O*-tetradecyl-3-*O*-β-D-glucosyl-*sn*-glycerol (14-Glc) with the phospholipids L-dimyristoylphosphatidylcholine (DMPC) and L-dimyristoylphosphatidylethanolamine (DMPE) were recorded by high-sensitivity differential scanning calorimetry and used for determination of the glycolipid–phospholipid miscibility in solid and liquid-crystalline states. As a consequence of a metastable behavior of both glycolipids and DMPE, the solid-state glycolipid/phospholipid miscibility was strongly dependent on the temperature prehistory of the samples. While DMPC and 14-Glc mix continuously, the other three binaries display extended regions of solid–solid-phase separation in the equilibrium low-temperature states. The DMPE/glycolipid phase diagrams were of clearly expressed eutectic type. Continuous solutions were formed in the liquid-crystalline and in the metastable solid phases of the mixtures. Simulations of the shape of the phase diagrams using the Bragg–Williams approximation showed certain deviations from ideal mixing in the liquid-crystalline continuous solutions. Since both glycolipids and phospholipids contain fully saturated fatty acids of equal chain length, their mixing properties were predominantly determined by the interactions between the lipid polar moieties, assuming the influence of ester or ether linkages of the alkyl chains on the mixing parameters to be negligible. The clearly expressed differences in the mixing of 14-Glc and 14-Gal with phospholipids are most probably due to different hydrogen-bond networks formed by the glucosyl and galactosyl residues.

The glycoglycerolipids constitute one of the major glycolipid classes. They are found in the membranes of plant cells (Sastry, 1974; Quinn & Williams, 1978), animal cells (Sweeley et al., 1977), and many kinds of bacteria (Ward, 1981; Boggs, 1980). Mostly present as minor lipid components, their amount in some membranes can reach remarkably high levels. Galactolipids, for example, represent up to 75% of the total lipid content in chloroplast membranes (Nishihara, 1980). Various functions have been proposed for these lipids, among them maintenance of membrane fluidity, modulation of protein conformations, and external membrane surface receptors (Ishizuka et al., 1985).

Much of the recent progress in the characterization of the structures formed by these amphiphiles in water has been made possible by development of methods for synthesis of stereochemically pure glycoglycerolipids of uniform fatty acid composition (Endo et al., 1982; Six et al., 1983). Application of NMR[1] (Jarrel et al., 1986), X-ray diffraction (Mannock et al., 1985), and DSC (Hinz et al., 1985) on pure glycoglycerolipid/water systems has revealed important aspects of their phase behavior and membrane-forming ability. Nevertheless, in comparison to phosphoglycerolipids, the phase properties of the glycoglycerolipids are less well understood although these lipids have identical lipophilic moieties. A main reason for this lack of understanding is the extreme diversity of the glycolipid carbohydrate composition, which results in a large variety of head groups of different size and polarity. The diversity of the carbohydrate moieties suggests an important contribution of the head-group interactions not only to the bilayer-forming ability of the various glycoglycerolipids but also to their interactions with other lipids and to their vectorial intramembrane localization.

† This article is dedicated to Julian Munson Sturtevant on the occasion of his eightieth birthday in admiration of his unceasing outstanding scientific activities and in gratitude for a long-standing friendship.
R.D.K. and B.G.T. are supported by the Bulgarian Academy of Sciences. H.L.K. and H.-J.H. are indebted to the Deutsche Forschungsgemeinschaft for supportive research grants. Collaborative research has been made possible on the basis of the Bulgarian–German scientific exchange program, and we express our gratitude to the Deutsche Forschungsgemeinschaft and to the Bulgarian Academy for mutual research stays in the laboratories in Sofia and Regensburg.
‡ Bulgarian Academy of Sciences.
§ Universität Regensburg.

[1] Abbreviations: 14-Gal, 1,2-di-*O*-tetradecyl-3-*O*-β-D-galactosyl-*sn*-glycerol; 14-Glc, 1,2-di-*O*-tetradecyl-3-*O*-β-D-glucosyl-*sn*-glycerol; DMPC, 1,2-dimyristoyl-*sn*-glycero-3-phosphocholine; DMPE, 1,2-dimyristoyl-*sn*-glycero-3-phosphoethanolamine; DPPC, 1,2-dipalmitoyl-*sn*-glycero-3-phosphocholine; L-DPPE, 1,2-dipalmitoyl-*sn*-glycero-3-phosphoethanolamine; DL-DPPE, *rac*-1,2-dipalmitoylglycero-3-phosphoethanolamine; DSC, differential scanning calorimetry; NMR, nuclear magnetic resonance.

0006-2960/88/0427-4612$01.50/0

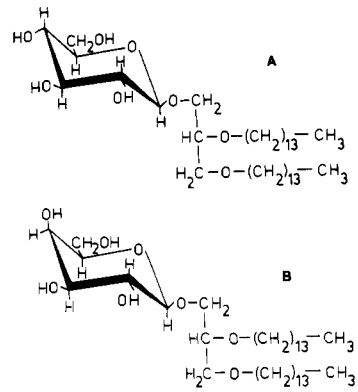

FIGURE 1: Structure of the synthetic glycolipids: (A) 1,2-di-*O*-tetradecyl-3-*O*-β-D-glucosyl-*sn*-glycerol; (B) 1,2-di-*O*-tetradecyl-3-*O*-β-D-galactosyl-*sn*-glycerol.

In order to gain some insight into the basis of these headgroup interactions, we have studied in the present work the mixing of glycoglycerolipids with phospholipids by analyzing the shape of their binary phase diagrams, which were recorded by means of high-sensitivity differential scanning calorimetry. The glycolipid and phospholipid species used contained fully saturated fatty acid chains of equal length (myristic acid) to eliminate the well-known effects on lipid mixing caused by fatty acid chain unsaturation and differences in chain length. Since the differences in physical behavior conferred upon lipids by ether and ester links are small (Ruocco et al., 1985; McKeone et al., 1986), variations of the mixing properties can therefore be considered as resulting practically entirely from the interactions between the lipid polar moieties.

The glycoglycerolipids used were synthetic, stereochemically pure compounds, 14-Glc and 14-Gal, containing in the carbohydrate domain monoglucosyl and monogalactosyl residues, respectively (Figure 1). These sugar residues occur frequently in glycoglycerolipids from natural sources. In animal cells the carbohydrate moieties of glycolipids are predominantly derived from Glc and Gal residues. Gal is also a ubiquituous component of plant cell glycolipids. The phospholipids used were DMPC and DMPE.

The thermodynamic parameters and mixing properties of the four glycolipid–phospholipid mixtures studied unexpectedly revealed great differences in the mixing of 14-Glc and 14-Gal with the two phospholipids in both solid and fluid states. The calorimetric results also showed the existence of metastable gel states of the mixtures, which are caused by the metastability of the pure lipid components.

Materials and Methods

Stereochemically pure 1,2-di-*O*-tetradecyl-3-*O*-β-D-glucosyl-*sn*-glycerol (14-Glc) and 1,2-di-*O*-tetradecyl-3-*O*-β-D-galactosyl-*sn*-glycerol (14-Gal) were synthesized according to a procedure described elsewhere (Six et al., 1983). Both glycolipids were chromatographically pure as checked by thin-layer chromatography. Stereochemical purity was checked by ^{1}H NMR at 250 MHz, which showed that the glycerol was linked via a β-glycosidic bond to the sugar residue. The phospholipids 1,2-dimyristoyl-*sn*-glycero-3-phosphocholine (DMPC) and 1,2-dimyristoyl-*sn*-glycero-3-phosphoethanolamine (DMPE) were obtained from Fluka AG and used without further purification. As tested by thin-layer and gas chromatography, they were at least 99% pure.

Appropriate amounts of phospholipid and glycolipid were mixed in chloroform or chloroform/methanol (2:1 v/v); the solvent was removed by rotary evaporation under nitrogen and the lipid mixture dried under vacuum for at least 6–8 h. Doubly distilled water was added to a lipid concentration of 0.25 mg/mL. The lipid dispersions were prepared by low-frequency sonication (22 kHz) for 20 min using a bath-type sonicator. In order to investigate the gel-state metastability of the lipids, the temperature during the sonication was kept either below (low-temperature treatment) or above (high-temperature treatment) the transition temperatures of the pure components. To retain the mixture of the liquid-crystalline phases resulting from the high-temperature treatment, the suspension temperature was quenched to 15 °C within 1 min. The suspension was then filled into the calorimeter, and the scan was started after approximately 20 min. This time lag between quenching of the lipid suspension and beginning of the calorimetric run is due to the equilibration time of the calorimeter after filling.

The thermograms were recorded with a high-sensitivity differential adiabatic scanning calorimeter (DASM-1M) at a 0.5 °C/min heating rate. The cooling of the sample inside the calorimetric cell between two successive heating runs is not controllable in a DASM-1M microcalorimeter. It obeys approximately an exponential law, and the time elapsing between the end of one scan and the start of the next scan was about 1 h for these measurements.

DSC measurements of dry glycolipids were performed with weighted lipid amounts (2 mg) in sealed aluminum pans. The thermograms were recorded with a Du Pont 1090 thermal analyzer supplied with a Du Pont 1091 disk memory at a heating rate of 2 °C/min. The cooling time between two successive heating scans was 10 min.

The characteristics of the phase transitions were determined in the standard way. The onset and completion temperatures of the phase transitions in the mixtures were used to construct the solidus and liquidus boundaries of the temperature–composition phase diagrams. The solidus and liquidus lines were corrected according to Lee (1977) to reduce the finite transition width of the pure components to isothermal melting.

Results

(*a*) *Gel-State Metastability of the Glycolipids and Their Mixtures with Phospholipids.* The four phospholipid/glycolipid mixtures studied were DMPC/14-Glc, DMPC/14-Gal, DMPE/14-Glc, and DMPE/14-Gal. The phase behavior of these mixtures was investigated on samples prepared at low and at high temperature (see Materials and Methods for details). The reason for using both low- and high-temperature treatments is that three of the pure lipid components, DMPE and both glycolipids, form metastable gel states when cooled from a liquid-crystalline state reached during a high-temperature treatment. Since the metastable states are relatively long-lived, samples of these lipids prepared at high and low temperatures are characterized by different patterns of phase transitions, at least during the first heating scan. Consequently, the phase diagrams of their mixtures with other lipids will also depend on the temperature history of the samples. The gel state of DMPC is also metastable, but only at prolonged exposure to temperatures below 10 °C (Finegold & Singer, 1986).

The gel-state metastability of DMPE is due to a low-temperature conversion of the metastable gel phase L_β into an equilibrium crystalline state, L_c (Mantsch et al., 1983). A sample of DMPE in excess water prepared at low temperature displays a single $L_c \rightarrow L_\alpha$ transition at 56 °C during the first heating scan, while a second scan following immediately after the first one, or after a high-temperature preparation of the sample, displays an $L_\beta \rightarrow L_\alpha$ transition at 49.3 °C (Figure 6a; Table I). The low-temperature conversion $L_\beta \rightarrow L_c$ is slow

Table I: Characteristics of the Phase Transitions of Pure Phospholipids and Glycolipids

lipid		I scan T_{tr} (°C)	I scan ΔH_{cal} (kcal/mol)	II scan T_{tr} (°C)	II scan ΔH_{cal} (kcal/mol)
14-Glc	dry	62.8	19.1	50.6	11.2
		113	0.1	113	0.1
	excess water	51.2	11.8	51.2	6.0
		56.0	1.2	56.0	1.2
14-Gal	dry	75.7	16.8		
		85.9	6.9	82.0	17.9
		128.0	0.3	128.0	0.3
	excess water	69.6	16.9	52.2	2.8
				69.6	3.8
DMPC	excess water	23.7	5.5	23.7	5.5
DMPE	excess water	55.8	13.9	49.3	4.6

enough so that during the cooling between two successive heating scans no detectable amount of the lipid converts to the L_c state. For this reason, it is possible to observe not only a pure $L_c \rightarrow L_\alpha$ transition but also a pure $L_\beta \rightarrow L_\alpha$ transition without the interference of the $L_c \rightarrow L_\alpha$ transition. The time required for complete $L_\beta \rightarrow L_c$ conversion of DMPE at 4 °C is about 6 days at 2 °C (Wilkinson & Nagle, 1984).

Basically, the metastability of 14-Gal is similar to that of DMPE, except for a more rapid low-temperature conversion of the metastable state into a stable one. Samples prepared at low temperature display a single transition at 70 °C in the first scan (Figures 4a, 6a; Table I), while during the second scan, this transition is strongly decreased in enthalpy and an additional peak appears at 52 °C (Figures 4a, 6a, 100% 14-Gal; Table I). Subsequent heating–cooling cycles do not further modify this picture.

The same pattern appears after a high-temperature sample preparation and also after a high-temperature incubation (above 70 °C) of the sample inside the calorimetric cell for 1 h. On the other hand, if during the cooling cycle after a heating scan the sample is incubated for 1 h at 15 °C before heating, then a subsequent heating scan will produce the original single transition at 70 °C, without traces of the low-temperature transition.

These observations show that the equilibrium low-temperature state of 14-Gal manifests itself through the transition at 70 °C, while the transition at 52 °C should be ascribed to a metastable gel state that appears during the cooling stage after a heating scan. Since the transition at 70 °C cannot be completely abolished by a high-temperature treatment, it appears that the time required for cooling between two successive heating runs is long enough to allow for a partial conversion of the metastable state into the stable one. This means, however, that binary mixtures with 14-Gal prepared at high temperature will actually convert to a mixture of "low-temperature" and "high-temperature" samples even before the first heating scan.

The glycolipid 14-Glc is also characterized by a metastable behavior. However, in this case the metastability is manifested only by an enthalpy decrease while the transition temperature remains the same (Figures 3a, 5a; Table I). Preliminary DSC measurements on shorter chain compounds (12-Glc and 10-Glc) show that the transition temperatures during first and second scans coincide only for the 14-Glc compound but not for the shorter chain compounds (Hinz et al., unpublished results). The conversion time of the metastable state into the initial equilibrium state is 72 h at 4 °C.

The gel-state metastability of the pure lipids results in differences in thermal behavior of their mixtures prepared at

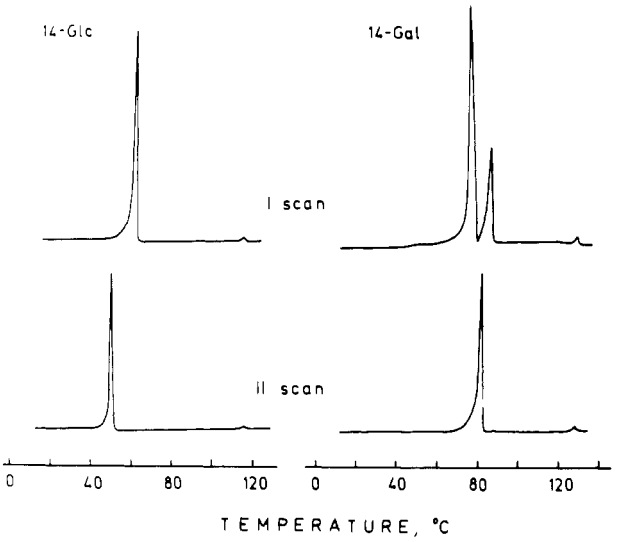

FIGURE 2: Thermograms of dry glycolipids in successive heating scans. Heating rate 2 °C/min; sample weight 2 mg; measurement in sealed aluminum pans.

low or high temperature. However, samples prepared at low temperature have different thermotropic properties in comparison to the high-temperature samples only during the first heating scan. Our experience with these mixtures shows that a low-temperature sample readily converts into a high-temperature sample during a calorimetric heating run (at a 0.5 °C/min heating rate), which proceeds to temperatures about 5–10 °C above the transition temperature of the highest melting pure lipid. The thermograms recorded during a successive second scan are practically identical with the first-scan thermograms of the corresponding high temperature samples. On the other hand, a 1-h incubation of a high-temperature sample of 14-Gal at 15 °C converts it back into a low-temperature sample.

In summary, the thermotropic behavior of the samples prepared at low temperature provides information about the lipid miscibility in the equilibrium low-temperature state, while the type of lipid mixing in the metastable gel states should be derived from the properties of the high-temperature samples.

In order to assess the effect of dispersing the glycolipids in aqueous medium, the phase transitions of dry glycolipids were also recorded (Figure 2). The transition characteristics are given in Table I. In the first scan dry 14-Glc melted at 62.8 °C with an enthalpy of 19.1 kcal/mol. In a successive second scan these values were reduced to 50.6 °C and 11.2 kcal/mol, respectively. Third scans performed 3 and 7 days after the second scans with samples kept at room temperature in the meantime showed a slow, monotonic recovery of the transition at 62.8 °C correlated with a decrease in enthalpy of the transition at 50.6 °C. Thus, it is evident that dry 14-Glc also can form a metastable solid state, similarly to 14-Glc dispersed in excess water.

Dry 14-Gal melted in two peaks during the first scan. In the second scan these two peaks merged into one transition centered at 82 °C with an enthalpy of 17.9 kcal/mol. We did not attempt to investigate the reason for the initial inhomogeneity in the preparation of crystalline 14-Gal. Both glycolipids also displayed small, reproducible posttransitions at significantly higher temperatures.

In summary, these data show that dispersing the glycolipids in excess water lowers either both transition temperature and enthalpy or at least one of these parameters. It can also be concluded that the method employed for preparation of the aqueous samples produces thermally homogeneous dispersions;

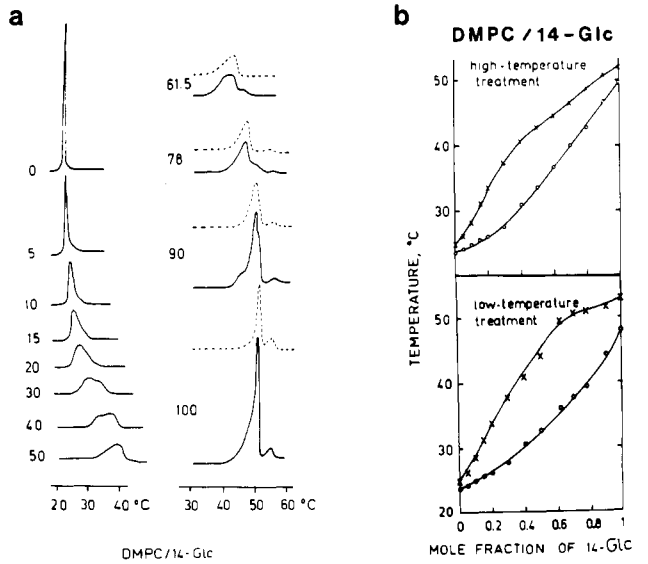

FIGURE 3: (a) DSC scans of mixtures of DMPC and 14-Glc: (—) low-temperature treatment (first scan); (---) high-temperature treatment (second scan). Solid and dashed lines coincide up to 50 mol % 14-Glc. (b) Temperature–composition phase diagrams of DMPC/14-Glc mixtures prepared at low and high temperatures: (O, ×) transition onset and completion, corresponding to solidus and liquidus lines, respectively.

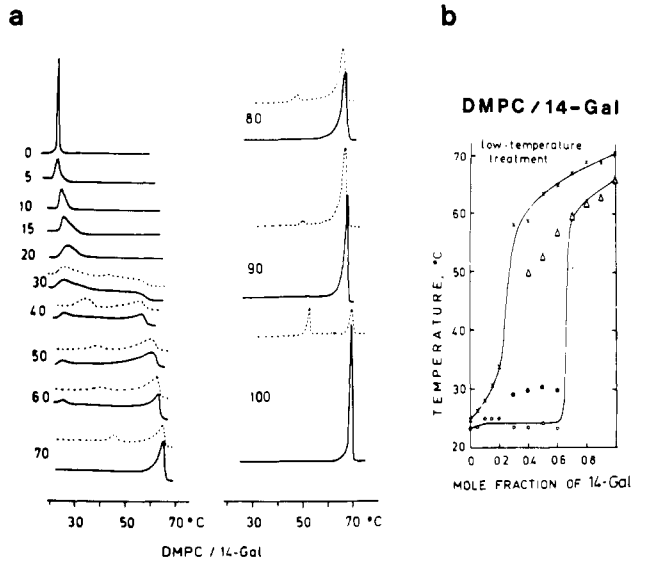

FIGURE 4: (a) DSC scans of mixtures of DMPC and 14-Gal. Notation as in Figure 3. Solid and dashed lines coincide up to 20 mol % 14-Gal. (b) Temperature–composition phase diagram of DMPC/14-Gal mixtures prepared at low temperature: (●, △); these symbols refer to points of completion and onset of the first and second peaks, respectively.

otherwise, heat capacity peaks characteristic of the dry glycolipids would have been detected in the aqueous dispersions.

(*b*) *Shape of the Phase Diagrams.* Sequences of DSC scans through the composition ranges of the four mixtures studied are shown in Figures 3a–6a. These scans were used to construct the solidus and liquidus lines of the temperature–composition phase diagrams of the lipid binary mixtures (Figures 3b–6b). The phase line originating from the 14-Glc post-transition at 56 °C is not shown in Figures 3b and 5b.

With respect to DMPC, the most interesting observation is that mixing of 14-Glc and 14-Gal with this phospholipid is qualitatively different. DMPC and 14-Glc form continuous solutions below and above the phase transition for samples prepared at both high and low temperatures (Figure 3a). The complete miscibility of these two lipids results in a lenslike

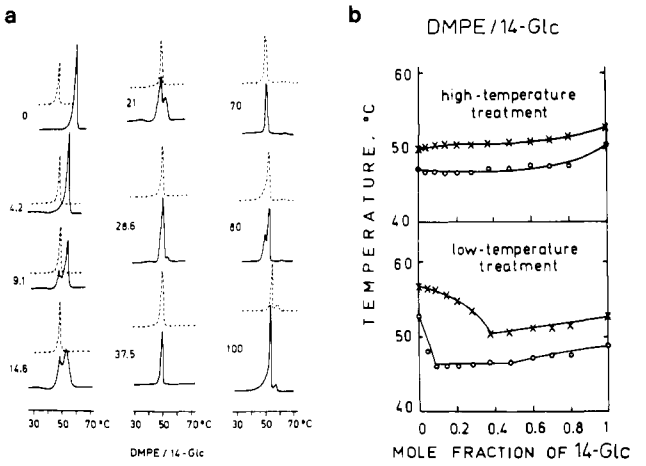

FIGURE 5: (a) DSC scans of mixtures of DMPE and 14-Glc. Notation as in Figure 3a. (b) Temperature–composition phase diagrams of DMPE/14-Glc mixtures prepared at low and high temperatures. Notation as in Figure 3b.

phase diagram, which indicates absence of regions of phase separation (Figure 3b). As will be shown further in the text, this conclusion is also confirmed by the results of a theoretical simulation of the shape of this phase diagram (Figure 7).

On the other hand, DMPC and 14-Gal are nearly completely immiscible in both gel and liquid-crystalline states (Figure 4a). The strongly restricted miscibility of these lipids is also evident in their phase diagram (Figure 4b). The horizontal portion of the solidus extends to at least 60 mol % 14-Gal, where it becomes unobservable. The transition of 14-Gal, which can be followed down to about 30 mol % of this component, markedly decreases in temperature. Phase behavior of this type indicates extended regions of solid–solid-phase separation and continuous miscibility in the fluid state of the mixtures.

After high-temperature treatment, the thermotropic behavior of the mixture becomes rather complicated due to the coexistence of stable and metastable phases of 14-Gal reflected in the splitting of its transition into two transitions at 52 and 70 °C [Figure 4a (dotted curves)]. Therefore, we did not try to construct high-temperature phase diagrams for the mixtures with 14-Gal. Nevertheless, the shift of the DMPC peak to higher temperatures at $X_{14\text{-Gal}} > 0.2$ is opposite to that found in the low-temperature thermograms, and it can be interpreted as an indication for better miscibility of DMPC with 14-Gal in the metastable solid state of the latter lipid than in its equilibrium solid state where the phase separation region is much more extended.

In comparison to the DMPC/14-Gal binary mixture, mixing of DMPE with 14-Gal is characteristically different. After a low-temperature preparation, mixtures of DMPE with 14-Gal display eutectic behavior with an eutectic point located at 52 °C and 0.2 mole fraction of 14-Gal (Figures 6b, 8). As is well-known from the theory of phase diagrams, eutectic behavior of the type illustrated in Figure 8 can appear if solid–solid-phase separation of the two components is associated with their complete miscibility in the fluid state. To our knowledge, this seems to be the first example of a lipid mixture showing clearly expressed eutectic behavior.

The low-temperature phase diagram of the DMPE/14-Glc mixture resembles a eutectic phase diagram but with a solidus line located very closely below the transitions of the pure components (Figure 5b, bottom).

Samples of DMPE and 14-Glc prepared at high temperature display phase transitions very similar in temperature and enthalpy (Table I). Their mixtures are characterized by phase

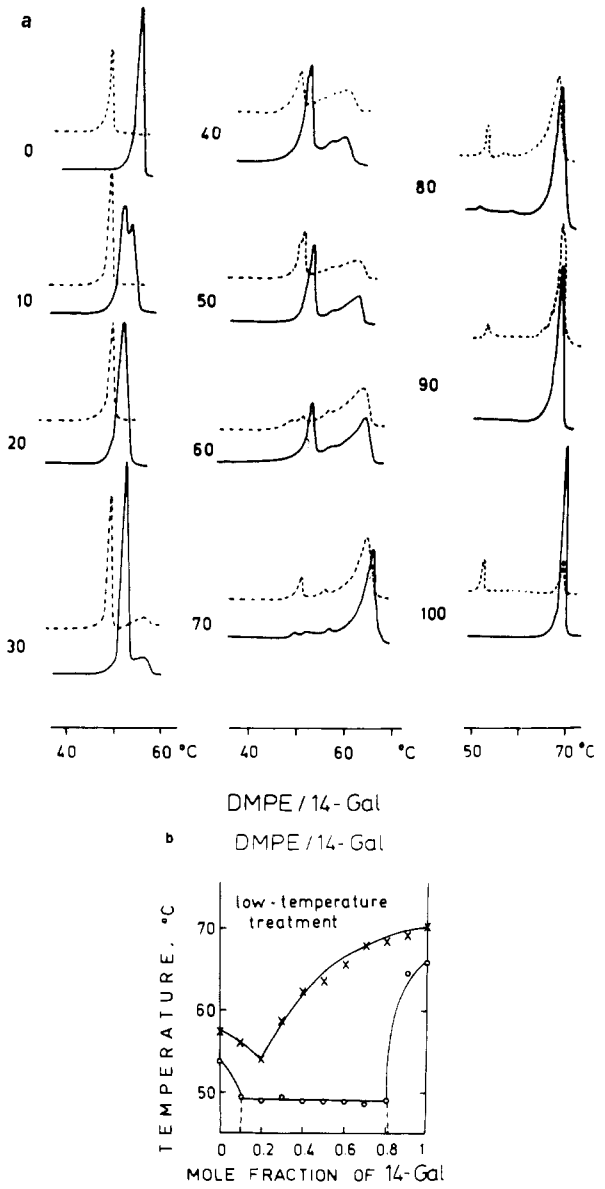

FIGURE 6: (a) DSC scans of mixtures of DMPE and 14-Gal. Notation as in Figure 3a. (b) Temperature–composition phase diagram of DMPE/14-Gal mixtures prepared at low temperature. Notation as in Figure 3b.

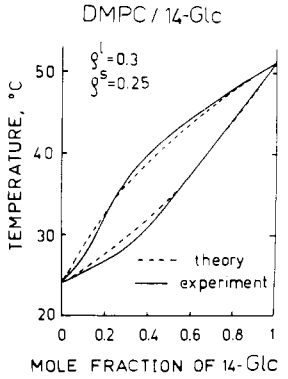

FIGURE 7: Corrected phase diagram of the DMPC/14-Gal mixture after high-temperature treatment constructed from Figure 2b, top (solid lines), and the best theoretical fit to it obtained with the Bragg–Williams approximation (dashed lines). The values of the nonideality parameters ζ^L and ζ^S are in kT units. Similar values also were obtained for the phase diagram in Figure 3b, bottom.

transitions that are practically indistinguishable from the transitions of the pure components (Figure 5a,b). Phase behavior of this type excludes eutectic, azeotropic, and other peculiar types of mixing that arise as a consequence of different lipid miscibilities in solid and liquid states. Only two alternative explanations are possible for the mixing properties of DMPE and 14-Glc: complete miscibility below and above the phase transition as opposed to complete solid–solid- and fluid–fluid-phase separations. We infer the former alternative, since the latter one seems unlikely for these compounds. Note that a solid–solid-phase separation combined with fluid miscibility would lead to eutectic behavior, which obviously is not the case observed.

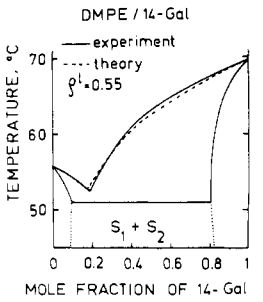

FIGURE 8: Corrected phase diagram for the DMPE/14-Gal mixture after low-temperature treatment constructed from Figure 6b, bottom (solid lines), and the best theoretical fit for the liquidus curve (dashed line). The nonideality parameter ζ^L is in kT units.

Simulation of the Phospholipid/Glycolipid Phase Diagrams. In a temperature–composition phase diagram, the solidus and liquidus curves enclose a region of equilibrium coexistence of solid and liquid phases. The principle of simulation of such diagrams follows directly from the conditions of thermodynamic equilibrium in a multicomponent, multiphase system, which require constant temperature and pressure throughout the system and equal chemical potentials of the components in the coexisting phases:

$$\mu_A^{S\circ} + \ln x_A^S + \ln f_A^S = \mu_A^{L\circ} + \ln x_A^L + \ln f_A^L$$
$$\mu_B^{S\circ} + \ln x_B^S + \ln f_B^S = \mu_B^{L\circ} + \ln x_B^L + \ln f_B^L \quad (1)$$

Here A and B denote phospholipid and glycolipid, respectively; S and L denote solid and liquid phase. The values of the standard chemical potentials, μ_A° and μ_B°, are related to the transition enthalpies, H_A and H_B, of the pure components through the Gibbs–Helmholtz equation:

$$\mu_A^{L\circ} - \mu_A^{S\circ} T_A = H_A(T_A - T)$$
$$\mu_A^{L\circ} - \mu_B^{S\circ} T_B = H_B(T_B - T) \quad (2)$$

Here T_A and T_B are the melting temperatures of the pure components.

In order to relate the activity coefficients, f_A and f_B, to the parameters of the lipid–lipid molecular interactions, we apply the Bragg–Williams approximation (mean field theory). In its frame f_A and f_B are given by (Hill, 1960)

$$\ln f_{A,B} = \zeta(1 - Z_{A,B})^2/kT \quad (3)$$

where $\zeta = ZE_{non}/2$ is an "energetic" nonideality parameter, k is the Boltzmann constant, T is the absolute temperature, Z is the number of nearest neighbors in lateral direction, and the nonideal energy of lateral interaction is defined as

$$E_{non} = 2E_{AB} - E_{AA} - E_{BB} \quad (4)$$

where E_{AB}, E_{AA}, and E_{BB} are the interaction energies of the three different kinds of nearest-neighbor pairs, AB, AA, and BB, respectively.

With the aid of eq 1 and 3, an experimental phase diagram can be simulated by varying ζ^S and ζ^L until the theoretical

Table II: Mixing Properties of Glycolipids and Phospholipids in Different Phases

	equilibrium solid phase	metastable solid phase	liquid-crystalline phase
DMPC/14-Glc	continuous solution, clustering of like lipids, $\zeta^S = 0.3kT$	continuous solution, clustering of like lipids, $\zeta^S = 0.25kT$	continuous solution, clustering of like lipids, $\zeta^L = 0.3kT$
DMPC/14-Gal	phase separation at $X_{Gal} \leq 0.6$		continuous solution[a]
DMPE/14-Glc	phase separation at $0.1 \leq X_{Glc} \leq 0.5$–$0.8$ (eutectics)	continuous solution	continuous solution
DMPE/14-Gal	phase separation at $0.1 \leq X_{Gal} \leq 0.8$ (eutectics)		continuous solution, clustering of like lipids, $\zeta^L = 0.55kT$

[a] The rather complex type of lipid mixing in this case cannot be determined with the aid of the Bragg–Williams approximation (see Simulation of the Phase Diagrams).

solidus and liquidus curves fit the experimental ones. The values of ζ^S and ζ^L obtained in this way characterize the lateral lipid ordering in the two phases. The value $\zeta = 0$ corresponds to ideal lateral mixing (ideal lenslike phase diagram), $\zeta > 0$ reflects clustering of the like lipids, which results in a true phase separation for ζ, $\zeta_c = kT/2X_AX_B$ (Lee, 1977; Tenchov, 1985), while $\zeta < 0$ reflects a "chessboard" arrangement of the two lipids (tendency to formation of compounds).

Due to its simplicity, the Bragg–Williams approximation has been frequently applied for analysis of phase diagrams of lipid mixtures (Lee, 1977; Tenchov, 1985, and references cited therein). Its major drawback is that a nonideality correction of the kind shown in eq 3 contributes only to the enthalpy term in the free energy of mixing, while the mixing entropy remains equal to that of an ideal mixture. Consequently, eq 3 reflects reality moderately well only at small deviations from ideality. Although the Bragg–Williams approach cannot be expected to be satisfactory in a quantitative way, it predicts correctly the most important qualitative features observed with binary solutions (Hill, 1960). Here we use it for characterization of the mixing in the continuous glycolipid–phospholipid solutions and determination of the regions of phase separation.

As is evident from the phase diagrams, continuous solutions are formed by the DMPC/14-Glc mixture below and above the phase transition (Figure 3b) and with the DMPE/14-Gal mixture above the melting transition (Figure 6b).

The best theoretical fits of the experimental solidus and liquidus curves are shown in Figures 7 and 8. The corresponding values of ζ^S and ζ^L are given in Table II. In all cases the values of ζ are positive but well below ζ_c ($0 < \zeta < \zeta_c$). This indicates deviations from ideal mixing behavior that are characteristic of clustering of the like lipids. The values of ζ also show an appreciably greater deviation from ideality for the fluid state of the DMPE/14-Gal mixture ($\zeta = 0.55kT$) than for the DMPC/14-Glc binary, which has similar mixing properties in gel and liquid-crystalline states ($\zeta^S \approx \zeta^L = 0.3kT$). However, in these cases the tendency of the like lipids to form clusters is not strong enough to interfere with their continuous mixing and to induce true phase separation. The DMPE/14-Glc binary most probably also forms continuous solutions, but due to the similarity of the enthalpies and transition temperatures of the pure lipids (Figure 5), the values of ζ cannot be determined in this case with sufficient precision.

The rather good quality of the fits in Figures 7 and 8 is a certain indication for the applicability of the Bragg–Williams approximation in these cases. On the other hand, the liquidus line of the DMPC/14-Gal phase diagram (Figure 4b) could not be satisfactorily simulated with any fixed pair of ζ^S and ζ^L. The principal obstacle is that this liquidus line is neither convex nor concave, but has a rather peculiar, sigmoidal shape. As a consequence, the value of ζ^L at low mole fractions of 14-Gal should be positive while at high mole fractions ζ^L changes sign and becomes strongly negative. For this reason, we are not able to present a consistent characterization of the lipid mixing in the DMPC/14-Gal mixture.

Phase separation in the mixtures is indicated by horizontal solidus and liquidus lines in the phase diagrams. In these cases the simulation of the phase diagrams produces values of ζ greater than the critical value, $\zeta_c = kT/2X_AX_B$ (Table II).

After low-temperature preparation, the mixtures DMPC/14-Gal, DMPE/14-Gal, and DMPE/14-Glc are characterized by extended regions of solid–solid-phase separation. The only exception was the DMPC/14-Glc binary, which formed continuous solid solutions also after low-temperature sample preparation (Table II).

Discussion

The main goal of the present study has been the characterization of the effects of polar head-group interactions on the mixing properties of phospholipid/glycolipid binary mixtures. Therefore, the four mixtures 14-Gal/DMPC, 14-Gal/DMPE, 14-Glc/DMPC, and 14-Glc/DMPE have been investigated after both a low- and a high-temperature preparation. Since the lipids contain identical saturated alkyl chains, differences in the shape of the phase diagrams can only result from differences in the interactions between the polar moieties of the lipids. The small contributions, resulting from the differences of ether and ester linkages, respectively, are of a different order of magnitude. The four mixtures studied are representative of different types of head-group interactions, which are known for their critical dependence on hydration (Curatolo, 1985; Maggio et al., 1985; Chang & Epand, 1983; Iwamoto et al., 1982). DMPC exhibits a bulky, charged head group with a moderate tendency for forming hydrogen bonds, while DMPE bilayers are characterized by extensive hydrogen-bond networks (Hauser et al., 1981). 14-Glc and 14-Gal are both uncharged lipids; the sugar head groups are stereoisomers differing only in the C-4 position hydroxyl group. In Gal the C-4 hydroxyl group assumes a vertical position; in Glc it is horizontal (Figure 1). Thus, formally, differences in the mixing properties and therefore in the interactions of the lipids can be assigned to this apparently minor stereochemical difference in the orientation of one C-4 hydroxyl group in the sugar head group.

It is known from previous studies (Hinz et al., 1985; Iwamoto et al., 1982) that synthetic glycolipids hydrate very poorly when dispersed in excess water. It is therefore of interest to compare the thermal behavior of dry glycolipids (crystalline powder obtained by recrystallization from methanol) with their dispersions in excess water. A similar comparison for L-DPPE and DL-DPPE, which also hydrate very poorly, shows that in the presence of excess water the crystal–liquid-crystalline transitions are lowered by 40 °C (Tenchov et al., 1984). In the case of DPPC, which can absorb large amounts of water, the melting phase transition is lowered from about 100 °C in the completely anhydrous state to 70–75 °C in the dihydrate and to 41 °C in the fully hydrated state (Kodoma et al., 1982).

However, the transition temperatures of 14-Glc and 14-Gal were lowered in excess water by not more than 10–12 °C (Table I). We take this to indicate a smaller degree of hydration than that observed with DPPC. This conclusion is also in accord with the theoretical estimates of the effect of hydration on the transition temperature of lipid bilayers (Cevc & Marsh, 1981, 1985). It appears therefore that the apparently greater thermal stability of the glycolipids in comparison to DMPC and DMPE in excess water should be attributed to a considerably lesser degree of hydration and not to an intrinsically greater stability of their anhydrous states.

The poor hydration of the glycolipids is probably related to the absence of electrostatic repulsion and also to the formation of a highly developed hydrogen-bond network between their polar moieties (Ruocco et al., 1981; Endo et al., 1982). This network might also be responsible for the different transitions of 14-Glc and 14-Gal in excess water (Table I). The phase transition of 14-Glc is of lower enthalpy and occurs at about 18 °C below the transition of 14-Gal. It appears that the different spacial orientation of the hydroxyl group at the C-4 position may result in different hydrogen bonding and, consequently, in different thermal stabilities of these two compounds. It is interesting to note in this context that pure galactose and glucose have different hydrogen-bonding numbers in aqueous solution (Savage & Wood, 1976; Barone et al., 1981).

The principal conclusions about the type of mixing in these four cases are summarized in Table II. They have been derived either directly from inspection of the phase diagrams of the mixtures or from theoretical simulations of their shape.

Especially when considering the solid-state miscibility of glycolipids and phospholipids, it is of principal importance to account for the strong dependence of the phase diagrams on the temperature prehistory of the samples. As shown under Results, this dependence originates from the formation of two types of solid phase (equilibrium and metastable) by DMPE and both the glycolipids. Therefore, it was necessary to distinguish between "equilibrium" and "metastable" lipid mixing at low temperatures. Experimentally, this was achieved by using low- and high-temperature regimes for sample preparation (Results). This approach was generally successful and allowed the demonstration of different lipid miscibilities in the equilibrium and metastable solid states.

Glycolipid dispersions equilibrated at low temperature are characterized by phase transitions of relatively large enthalpies (Table I). On the other hand, when cooled from the liquid-crystalline phase they form metastable solid states. Taking into account similar experiences with other lipids (Chang & Epand, 1983; Mantsch et al., 1983; Seddon et al., 1983), these observations provide sufficient evidence to conclude that the equilibrium low-temperature states are crystalline phases that transform directly into the liquid-crystalline phase upon heating. Our preliminary X-ray observations confirm this interpretation (unpublished results). Since formation of crystalline phases would most probably interfere with mixing of glycolipids and phospholipids, it is not surprising that three of the mixtures studied (DMPC/14-Gal, DMPE/14-Gal, and DMPE/14-Glc) have extended regions of solid–solid-phase separation after low-temperature equilibration (Table II). While DMPE forms eutectic mixtures with both glycolipids (Figures 5b, 6b), the type of phase separation in the DMPC/14-Gal binary is not clearly expressed in the transition curves and therefore cannot be determined from its phase diagram (Figure 4b). On the other hand, the DMPC/14-Glc binary did not phase-separate but formed continuous solutions in the equilibrium solid state (Figure 3b).

These data show a drastic influence of both glycolipid and phospholipid head groups on the equilibrium solid-state miscibility of the lipids. Thus, replacement of 14-Gal with 14-Glc in mixtures with DMPC and of DMPE with DMPC in mixtures with 14-Glc leads to transformation of phase-separated regions into continuous solutions. A strong effect on the phase diagram is also exerted by the replacement of DMPE with DMPC in mixtures with 14-Gal (Figures 4b, 6b). The only pair of mixtures with comparable properties is the mixtures of DMPE with 14-Gal and 14-Glc, where eutectic phase diagrams have been observed (Figures 5b, 6b).

In the liquid-cyrstalline phases continuous solutions of all four mixtures were formed. However, as shown by the simulations of the phase diagrams, there are certain deviations from ideal mixing even in the liquid-crystalline phases of the mixtures. These deviations were expressed to a different degree for the different mixtures. For example, clustering of the like lipids is more pronounced in the liquid-crystalline phase of the DMPE/14-Gal binary than in the DMPC/14-Glc binary (Figures 7, 8; Table II).

In summary, the DSC data clearly show that even very small variations in the head groups of both phospholipids and glycolipids have profound effects on their mutual miscibility in both solid and liquid-crystalline states. These findings may be of importance for an understanding of biological membranes where the functional significance of the large variety of lipid head groups in general and the role of glycolipids in particular are well recognized but poorly understood. Alterations in mixing properties with concomitant domain formation as a function of head-group composition can well be envisaged as being instrumental in modifying the dynamic properties of biological membranes.

References

Barone, G., Cacace, P., Castronuovo, G., & Elia, V. (1981) *Carbohydr. Res. 91*, 101–111.

Boggs, J. M. (1980) *Can. J. Biochem. 58*, 755–770.

Cevc, G., & Marsh, D. (1981) *Period. Biol. 83*, 118–120.

Cevc, G., & Marsh, D. (1985) *Biophys. J. 47*, 21–31.

Chang, H., & Epand, R. M. (1983) *Biochim. Biophys. Acta 728*, 319–324.

Curatolo, W. (1985) *Biochim. Biophys. Acta 817*, 134–138.

Endo, T., Inoue, K., & Nojima, S. (1982) *J. Biochem. (Tokyo) 92*, 953–960.

Finegold, L., & Singer, M. A. (1986) *Biochim. Biophys. Acta 855*, 417–420.

Hauser, H., Pascher, I., Pearson, R. H., & Sundell, S. (1981) *Biochim. Biophys. Acta 650*, 21–51.

Hill, T. L. (1960) *Introduction to Statistical Thermodynamics*, Addison-Wesley, Reading, MA.

Hinz, H.-J., Six, L., Ruess, K.-P., & Liefländer, M. (1985) *Biochemistry 24*, 806–813.

Ishizuka, I., & Yamakaiva, T. (1985) in *Glycolipids* (Wiegandt, H., Ed.) Elsevier and Academic, New York.

Iwamoto, K., Sunamoto, J., Inoue, K., Endo, T., & Nojima, S. (1982) *Biochim. Biophys. Acta 691*, 44–51.

Jarrel, H. C., Giziewicz, J. B., & Smith, J. C. P. (1986) *Biochemistry 25*, 3950–3957.

Kodoma, M., Kuwabara, M., & Seki, S. (1982) *Biochim. Biophys. Acta 689*, 567–570.

Lee, A. G. (1977) *Biochim. Biophys. Acta 472*, 285–344.

Maggio, B., Ariga, T., Sturtevant, J. M., & Yu, R. K. (1985) *Biochemistry 24*, 1084–1092.

Mannock, D. A., Brain, A. P. R., & Williams, W. P. (1985) *Biochim. Biophys. Acta 817*, 289–298.

Mantsch, H. H., Hsi, S. C., Butler, K. W., & Cameron, D. G. (1983) *Biochim. Biophys. Acta 728*, 325–330.
McKeone, B. J., Pownell, H. J., & Massey, J. B. (1986) *Biochemistry 25*, 771–7716.
Nishihara, M., Yokata, K., & Kito, M. (1980) *Biochim. Biophys. Acta 617*, 12–19.
Quinn, P. J., & Williams, W. P. (1978) *Prog. Biophys. Mol. Biol. 34*, 109–179.
Ruocco, M. J., Atkinson, D., Small, D. M., Skarjune, R. P., Oldfield, E., & Shipley, G. G. (1981) *Biochemistry 20*, 5957–5966.
Ruocco, M. J., Siminovitch, D. J., & Griffin, R. G. (1985) *Biochemistry 24*, 2406–2411.
Sastry, P. S. (1974) *Adv. Lipid Res. 12*, 251–310.
Savage, I. I., & Wood, R. H. (1976) *J. Solution Chem. 5*, 733–750.
Seddon, J. M., Harlos, K., & Marsh, D. (1983) *J. Biol. Chem. 258*, 3850–3854.
Six, L., Ruess, K.-P., & Liefländer, M. (1983) *Tetrahedron Lett. 24*, 1229–1232.
Sweeley, C. C., & Siddiqui, B. (1977) in *Glycoconjugates* (Horrowitz, M. J., & Pigman, W., Eds.) Vol. 1, pp 459–540, Academic, New York.
Tenchov, B. G. (1985) *Progress Surf. Sci. 20(4)*, 273–340.
Tenchov, B. G., Boyanov, A. I., & Koynova, R. D. (1984) *Biochemistry 23*, 3553–3558.
Ward, J. B. (1981) *Microbiol. Rev. 45*, 211–243.
Wilkinson, D. A.; & Nagle, J. F. (1984) *Biochemistry 23*, 1538–1541.

Phospholipids Chiral at Phosphorus. Synthesis and Stereospecificity of Phosphorothioate Analogues of Platelet-Activating Factor†

Theresa Rosario-Jansen, Ru-Tai Jiang, and Ming-Daw Tsai*
Department of Chemistry, The Ohio State University, Columbus, Ohio 43210
Donald J. Hanahan*
Department of Biochemistry, The University of Texas Health Center at San Antonio, San Antonio, Texas 78284
Received November 20, 1987; Revised Manuscript Received February 9, 1988

ABSTRACT: R_P and S_P isomers of 1-*O*-hexadecyl-2-acetyl-3-thiophosphocholine (AGEPsC) have been synthesized. The activity of these isomers in platelet aggregation and serotonin secretion was compared with that of 1-*O*-hexadecyl-2-acetyl-3-phosphocholine (AGEPC). The results show that (S_P)-AGEPsC has the same activity as AGEPC within experimental error in both assays. The R_P isomer, however, is only 0.6–2% as active as AGEPC in platelet aggregation and serotonin release. The results suggest that the phosphate group of AGEPC is likely to be involved in the interactions with its receptor, at least in the events leading to platelet aggregation and secretion.

Platelet-activating factor (PAF)[1] is a naturally occurring simple phosphoglyceride with very potent biological activity (Snyder, 1986; Hanahan, 1986; Hanahan & Kumar, 1987). Its existence was first suggested by Henson (1970), Sirganian and Osler (1971), and Benveniste et al. (1972), but the exact chemical structure of the naturally occurring compound was not deduced until 10 years later (Hanahan et al., 1980). As shown in Figure 1, the structure of natural PAF is 1-*O*-alkyl-2-acetyl-*sn*-glycero-3-phosphocholine (AGEPC), with the alkyl chain varying from C14:0 to C18:1.

Since its discovery, an enormous research effort has been focused on elucidating the biochemical nature of PAF. It is the first example of a phosphoglyceride with biological activity, apart from the familiar role as a structural entity in biological membranes. It is a potent mediator of many biological processes, having roles in antihypertensive activity, cardiovascular effects, bronchoconstriction, and immunopathological response [see reviews, Hanahan (1986) and Hanahan and Kumar (1987)]. To date, it is the most potent known activator of platelets, causing them to degranulate and aggregate at concentrations as low as 10^{-10} M in washed rabbit platelets.

The structural features important to the biological activity of this unique phosphoglyceride have been explored in depth by many laboratories, especially relative to substituents at the *sn*-1 and *sn*-2 positions. Consequently, only a few selective

† This work was supported by National Institutes of Health Research Grant GM 30327 (to M.-D.T) and Welch Foundation Grant AQ 887 (to D.J.H). The Bruker AM-500 NMR spectrometer used was partially funded by NIH Grant RR 01458. M.-D.T. is a Camille and Henry Dreyfus Teacher–Scholar, 1985–1990. Preliminary results of this work have been presented at the 2nd International Conference on Platelet Activating Factor, Gatlinburg, TN, Oct 26–29, 1986, and at the 10th International Conference on Phosphorus Chemistry, Bonn, West Germany, Aug 31–Sept 6, 1986. This is paper 16 in the series "Phospholipids Chiral at Phosphorus". For paper 15, see Raetz et al. (1987).

[1] Abbreviations: AGEPC, 1-*O*-alkyl-2-acetyl-*sn*-glycero-3-phosphocholine; AGEPsC, 1-*O*-hexadecyl-2-acetyl-*sn*-glycero-3-thiophosphocholine; CDMP, chloro(*N*,*N*-diisopropylamino)methoxyphosphine; DMAP, 4-(*N*,*N*-dimethylamino)pyridine; DPPC, 1,2-dipalmitoyl-*sn*-glycero-3-phosphocholine; DPPsC, 1,2-dipalmitoyl-*sn*-glycero-3-thiophosphocholine; lyso-GEPC, 1-*O*-alkyl-2-lyso-*sn*-glycero-3-phosphocholine; lyso-GEPsC, 1-*O*-hexadecyl-2-lyso-*sn*-glycero-3-thiophosphocholine; PAF, platelet-activating factor; PLA2, phospholipase A_2; PLC, phospholipase C; TBAH, tetrabutylammonium hydroxide; Tris, 2-amino-2-(hydroxymethyl)-1,3-propanediol; EDTA, ethylenediaminetetraacetate.

0006-2960/88/0427-4619$01.50/0